

Luttinger Liquid State with Effective Attractive Hard-Core Interaction

Igor N. Karnaukhov^{1,2}

¹Max-Planck-Institut für Physik komplexer Systeme, Nöthnitzer Straße 38, 01187 Dresden, Germany

²Institute of Metal Physics, Vernadsky Street 36, 03142 Kiev, Ukraine

An exact solvable 'zig-zag' ladder model of degenerated spinless fermions is proposed and solved exactly by the means of the Bethe ansatz. An effective attractive hard-core interaction and direct Coulomb repulsion of fermions on the nearest-neighbor sites of different chains induce a new phase state of the ladder. We give a detailed analysis of the exact phase diagram at zero temperature, that is characterized by two phases at the filling exceeding 2/3: itinerant and 'frozen' fermions, for which two different species reside in spatially separate regions. The critical exponents describing asymptotic behavior of the correlation functions are calculated using the Bethe ansatz and conformal field theory. It is shown also, that the density of the magnetization of the corresponding zig-zag spin-1/2 ladder has a jump equal to 1/3 at the magnetic field equal to zero.

PACS numbers: 71.10.Fd; 71.10.Pm

The metallic single-walled carbon nanotubes (SWNT's) represent one-dimensional (1D) systems (in the sense of their electronic properties), in which one may expect to observe physical phenomena characteristic for strong electron correlations. Informer studies attention has been mostly concentrated on the realization of the Tomonaga-Luttinger liquid state in these systems. This conclusion follows from the analysis of their transport properties^{1,2} and from the direct observation of electronic states near the Fermi energy in the high-resolution photoemission experiments³. The large value of the critical exponent Θ ($\Theta = 0.3 - 0.5^{1,2,3}$), extracted from the experimental results, which describes the asymptotic behavior of the spectral function near the Fermi energy, indicates that large density-density correlations dominate in the system. In other words, SWNT's are 1D electronic systems with strong repulsive interaction between fermions. The strong correlations work wonders in such electron liquid, therefore a traditional Luttinger liquid approach⁴ that is relevant in the case of a weak electron-electron interaction can not explain the mechanism of interactions inherent in carbon nanotubes⁵. It is necessary to use exactly solvable models or numerical calculations of many-body fermion systems with strong interactions for the complete understanding of such intriguing behavior of SWNT's. We shall exploit this conception and develop an approach based on the exact solvable zig-zag ladder model of spinless fermions. An effective attractive hard-core and direct repulsive interactions are intrinsic in the model considered. As it will be shown below, the interplay of these interactions gives a rise to the phase diagram, which includes interesting strongly correlated states of fermions at the high filling. The values of Θ calculated in the framework of the model proposed are in qualitative agreement with Ref.^{1,2,3}.

The metallic state of SWNT's is realized in the two possible high symmetry structures for nanotubes, known as zig-zag and 'armchair' ($m = 0$ for all zig-zag tubes while $n = m$ for all armchair tubes⁶). The coupled chains in the form of the ladders are hard lattice mod-

els of strongly correlated systems exactly solvable in uncommon cases. Indeed, such systems are frequently frustrated⁷. The models of the coupled spin chains⁸ and spin ladders have been studied intensively^{9,10,11}. Nevertheless, there are still many open questions on the gaps in the spectrum of collective excitations and the behavior of these systems away from half-filling. In this Letter we consider the model for zig-zag nanotubes in the form of the zig-zag ladder of degenerated spinless fermions taking into account the hopping of fermions along the chains and the interaction between fermions on the nearest-neighbor lattice sites of different chains. The model Hamiltonian is given by

$$\mathcal{H} = - \sum_j (c_j^\dagger c_{j+1} + c_{j+1}^\dagger c_j) (1 - n_{j+\frac{1}{2}}) - JN + \epsilon_1 M_1 + \epsilon_2 M_2 + \frac{1}{2} J \sum_j (n_j + n_{j+1}) n_{j+\frac{1}{2}}, \quad (1)$$

where c_j and c_j^\dagger are operators of spinless fermions at site j shifted on a half-lattice constant for different chains, accordingly the first and the second chains, the hopping integral is equal to unity, ϵ_1 and ϵ_2 define a relative shift of the fermion subbands of the chains, J is the repulsion interaction of fermions on the nearest-neighbor sites of different chains, the particle number operator for fermions is defined by $n_j = c_j^\dagger c_j$. The summation extends over all sites of the chains of the length L , we assume periodic closure. The hopping of fermions through the sites occupied by fermions of another chain is forbidden in the hopping term of the Hamiltonian. The Hamiltonian conserves the total number of fermions of each chain M_1 and M_2 , $N = M_1 + M_2$ is the total number of particles. At $\epsilon_1 = \epsilon_2$ the chains are identical and the Hamiltonian (1) is reduced to the zig-zag spin-1/2 ladder in the magnetic field $H = \epsilon_1 \mathcal{H} = - \sum_j (S_j^x S_{j+1}^x + S_j^y S_{j+1}^y) (S_{j+\frac{1}{2}}^z + 1/2) - H \sum_j S_j^z + \frac{1}{2} J \sum_j (S_j^z + S_{j+1}^z) S_{j+\frac{1}{2}}^z$. By way of illustration of the structure of the zig-zag ladder and interaction the chains are shown in Fig. 1.

We now turn to the diagonalization of the model

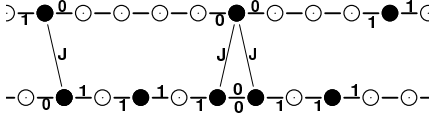


FIG. 1: Graphical representation of the zig-zag ladder; 0 and 1 denote the value of the hopping integral along the chains between the nearest-neighbor sites at given configuration of fermions.

Hamiltonian by the coordinate Bethe ansatz formalism. The Schrödinger equation is solved with the ansatz

$$\psi(x_1, x_2, \dots, x_N) = \sum_P (-1)^P A(P) \exp\left(i \sum_{j=1}^N k_{Pj} x_j\right), \quad (2)$$

where the P summation extends over all the permutations of the momenta $\{k_j\}$ of the particles.

According to the form of the interaction in (1) the fermions of one chain are scattered on the fermions of another only, the two-particle scattering matrix of the spinless fermions with momenta k_i and k_j is given by $S_{ij} = \exp\left[\frac{i}{2}(k_i - k_j)\right] \frac{1 + \exp[i(k_i + k_j)] + J \exp(ik_j)}{1 + \exp[i(k_i + k_j)] + J \exp(ik_i)}$. An additional constrain on the form of the interaction in (1) follows from the calculations of the configurations with three particles in different chains on the neighboring lattice sites (it is sketched in Fig. 1). Direct calculations show that if the model Hamiltonian (1) does not contain a direct interaction of fermions on the nearest-neighbor sites of the same chain (when the site between these particles is occupied), the relation between amplitudes of the three-particle wave function holds for arbitrary configuration of the particles $A(k_{P'1}, k_{P'2}, k_{P'3}) = S(k_{Pj}, k_{Pj+1})A(k_{P1}, k_{P2}, k_{P3})$ (here P is an arbitrary permutation and $P' = P(j, j+1)$).

The energy eigenstates are characterized by sets of the charge rapidities $\{\lambda_j\}$ ($j = 1, \dots, N$) for the particles, that satisfy the following Bethe equations written below in the case of a weak interaction $J/2 = \cos \eta < 1$ for the charge rapidities of the 1-st chain ($\{\lambda_j\}$, $j = 1, \dots, M_1$)

$$\left[\frac{\sinh \frac{1}{2}(\lambda_j + i\eta)}{\sinh \frac{1}{2}(\lambda_j - i\eta)} \right]^{L + \frac{1}{2}M_2} = \exp\left(\frac{1}{2}\mathcal{P}_2\right) \prod_{i=1}^{M_2} \frac{\sinh \frac{1}{2}(\lambda_j - \lambda_i + 2i\eta)}{\sinh \frac{1}{2}(\lambda_j - \lambda_i - 2i\eta)}, \quad (3)$$

where $\exp(ik_j) = \frac{\sinh \frac{1}{2}(\lambda_j + i\eta)}{\sinh \frac{1}{2}(\lambda_j - i\eta)}$, $\mathcal{P}_2 = \sum_{i=1}^{M_2} k_i$ is the momentum of the 2-nd chain. The eigenenergy of the ladder is defined by $E = -2 \sum_{j=1}^N \cos k_j + \epsilon_1 M_1 + \epsilon_2 M_2$. The charge rapidities of the 2-nd chain are solutions of the similar Bethe equations.

The fillings of the fermionic subbands are defined by the chemical potential of the system, which is the same for different subbands at their partial filling, thus $M_1 = M_2$ at $\epsilon_1 = \epsilon_2$ for identical chains. In the thermodynamic

limit the rapidities λ_j are closed spaced and may be regarded as continuous variable. The distribution functions of the charge rapidities $\rho_{1,2}(\lambda)$ for each chain are defined through the integral equations of the Fredholm type

$$\rho_{1,2}(\lambda) + \int_{-\Lambda_{2,1}}^{\Lambda_{2,1}} d\lambda' R_2(\lambda - \lambda') \rho_{2,1}(\lambda') = (1 + m_{2,1}/2) R_1(\lambda), \quad (4)$$

with the kernel $R_n(\lambda) = \frac{1}{2\pi} \frac{\sin(n\eta)}{\cosh \lambda - \cos(n\eta)}$, $m_{1,2} = M_{1,2}/L = \int_{-\Lambda_{1,2}}^{\Lambda_{1,2}} d\lambda \rho_{1,2}(\lambda)$ are the densities of fermions in the chains, $\epsilon_{1,2} = m_{1,2} \epsilon_{1,2} - 4\pi \sin \eta \int_{-\Lambda_{1,2}}^{\Lambda_{1,2}} d\lambda R_1(\lambda) \rho_{1,2}(\lambda)$ are the densities of the ground-state energy of the chains. The similar Bethe equations take place in the case of a strong repulsive interaction at $J/2 = \cosh \mu \geq 1$. The corresponding integral equations are defined by the kernel $R_n(\lambda) = \frac{1}{2\pi} \frac{\sinh(n\mu)}{\cosh(n\mu) - \cos \lambda}$.

The low-density region of the phase diagram, when the distance between particles is large compared to the hard-core radius, describes itinerant fermions in the Coulomb potential J , since an effective force of the the hard-core interaction is insignificant. Complicated physical picture arises in region of high densities of fermions, since radically different situation is realized in the model at high filling of the chains when the average distance between particles is compared with the hard-core radius and the hard-core interaction dominates. The integral equations (4) are defined for the density of particles less than a 'half-filling' equaled to $2/3$ for identical chains. For investigation of fermionic states of the ladder at larger filling let us use the combined electron-hole symmetry $c_j \rightarrow (-1)^j c_j^\dagger$ for the Hamiltonian (1) and obtain $\mathcal{H} \rightarrow \mathcal{H}'$

$$\mathcal{H}' = \sum_j [-c_j^\dagger c_{j+1} - c_{j+1}^\dagger c_j + \frac{1}{2}J(n_j + n_{j+1})] n_{j+\frac{1}{2}} - JN + \epsilon_1(L - M_1) + \epsilon_2(L - M_2). \quad (5)$$

The Hamiltonian (5) describes the hole states in the ladder, whereas the fermion states of the first and hole states of the second chains are defined by the following Hamiltonian

$$\mathcal{H}' = - \sum_{j=1}^L (c_j^\dagger c_{j+1} + c_{j+1}^\dagger c_j) n_{j+\frac{1}{2}} + (\epsilon_1 + J)M_1 - \sum_{j=1/2}^L (c_j^\dagger c_{j+1} + c_{j+1}^\dagger c_j)(1 - n_{j+\frac{1}{2}}) + (\epsilon_2 - J)(L - M_2) - \frac{1}{2}J \sum_j (n_j + n_{j+1}) n_{j+\frac{1}{2}}. \quad (6)$$

The phase state of the model is result of the interplay of the repulsive Coulomb interaction J and effective attractive hard-core interaction with a negative hard-core

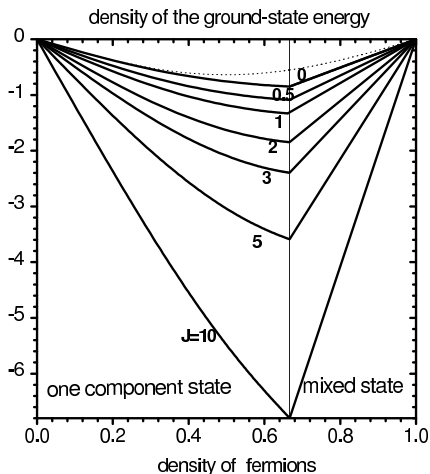


FIG. 2: Ground-state energy as a function of the density of spinless fermions. Individual curves are labelled by value of $J=0;0.5;1;2;3;5;10$, a dotted curve corresponds to free fermion state.

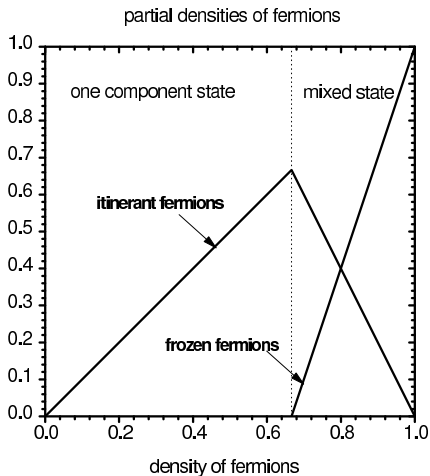


FIG. 3: Phase diagram in the coordinates of the densities of itinerant and frozen fermions as a function of the density of fermions.

radius equaled to $-1/4$. We shall show, that phase separation occurs at high densities of particles ($n > 2/3$). First of all let us answer on the question: *what is it the effective attractive hard-core interaction?* A repulsive hard-core interaction forbids two particles being at distances less or equal to doubled hard-core radius l , that corresponds to equaled to zero two-particle wave function $\psi(x_i, x_j)$ at $|x_j - x_i| \leq l$. The interaction in the Hamiltonian (1) forbids the tunneling of particles of different chains on distance of a half-lattice constant, other words the two-particle wave function is equal to zero after the result of the hopping (or the current is equal to zero), then $\psi(x, x) \neq 0$ automatically in the case for a nontrivial solution for the wave function. Thus this condition on the two-particle wave function leads to an effective attraction between two particles of different chains with

the same coordinates in contrast to a traditional repulsive hard-core interaction for that $\psi(x_j, x_j) = 0$.

Using exact solutions of the Hamiltonians (5),(6) we can calculate the phase diagram at arbitrary fillings of the chains, below we consider identical chains. The Hamiltonians (5) is defined the phase state of fermions with frozen hopping. The Bethe function (2) is the solution of the Schrödinger equations with equaled to zero energy and the two-particle scattering matrix $S'_{ij} = \exp[\frac{i}{2}(k_j - k_i)]$. Really this phase corresponds to full-filled states of the chains, other words these solutions describe the phase separation of the chains at $n > 2/3$: the full-filled states of fermions in the chains with frozen hoppings and the 'old' phase of itinerant fermions defined by the Bethe equations (3) on the restricted chains. The density of the ground-state energy is plotted in Fig. 2 at $\epsilon_1 = \epsilon_2 = 0$. At $n > 2/3$ the density of 'frozen' fermions is equal to $\delta n = 3n - 2$, the corresponding density of the itinerant fermions $\Delta n = n - \delta n = 2(1 - n)$ (see Fig. 3). In a separate point $J \rightarrow \infty$ the scattering matrix is defined by conditions $\psi(x_{j \pm \frac{1}{2}}, x_j) = 0$, that corresponds to a constrain on the tree-particle wave function $\psi(x_{j+1}, x_{j+\frac{1}{2}}, x_j) = 0$ also, therefore the maximal filling of chains is equal to $1/3$. In the case of a strong repulsive interaction $J > 2$ both phases are dielectric, the phase of itinerant fermions is metallic for a weak interaction $J \leq 2$.

The Luttinger liquid parameter $K_\rho^{1,2}$ is defined by the dressed charge $\chi_{1,2}(\Lambda)$ via $K_\rho^{1,2} = \chi_{1,2}^2(\Lambda)$. The integral equations for the dressed charge functions $\chi_{1,2}(\lambda)$ is distinguished from equations (4) by the driving term

$$\chi_{1,2}(\lambda) + \int_{-\Lambda_{2,1}}^{\Lambda_{2,1}} d\lambda' R_2(\lambda - \lambda') \chi_{2,1}(\lambda') = (1 + m_{2,1}/2). \quad (7)$$

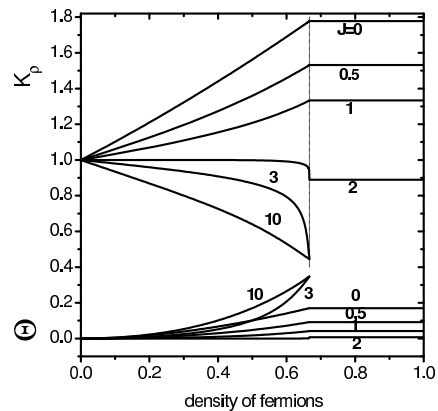


FIG. 4: The critical exponents K_ρ and Θ at $J=0;0.5;1;2;3;10$.

According to (7) the repulsive interaction J decreases the value of K_ρ . In contrast to traditional hard-core interaction, that decreases the value of K_ρ extremely⁵, an effective attractive hard-core interaction increases K_ρ . The low density limit $m_{1,2} \rightarrow 0$ corresponds to free spinless fermions with $K_\rho \rightarrow 1$. In the case of the identical

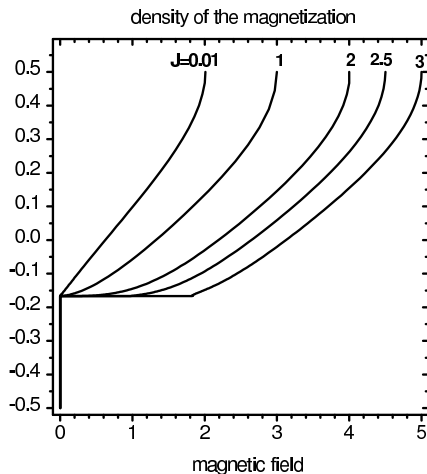


FIG. 5: Density of the magnetization of the spin ladder model as a function of the magnetic field at $J=0.01$; 1; 2; 2.5; 3.

chains the system of integral equations (7) is reduced to one and we obtain the solution for $K_\rho = \frac{8}{9} \frac{\pi}{\pi - \eta}$ at half filling $m_{1,2} = 2/3$ using the Wiener-Hopf method. The maximal value of $K_\rho = 16/9$ is realized in the $J \rightarrow 0$ limit, that corresponds to $\Theta = 0.17$. The critical exponent Θ is related to the Luttinger parameter K_ρ through $\Theta = (K_\rho - 2 + 1/K_\rho)/2$. Whereas, the minimal value $K_\rho = 4/9$ is obtained in the $J \rightarrow \infty$ limit, we have twice larger value of the critical exponent $\Theta = 0.35$ in this case. Numerically solving integral equations (4),(7) we calculate the critical exponents K_ρ and Θ for each chain as function of the density of spinless fermions for different values of J . Numerical calculations of the exponents are shown in Fig. 4 for illustration of the behavior of the critical exponents for arbitrary densities of particles and interaction. In an effective attractive regime at a weak interaction ($J < 2$) the value of K_ρ decreases from $16/9$ to 1 with increasing J from 0 to $J = J_0$ (the value of K_ρ depends of the density fermions therefore J_0 depends of n also, according to simulations $1.7 < J_0 < 1.9$), whereas

the value of Θ decreases from 0.17 to zero. The phase of itinerant fermions is metallic at $n > 2/3$, therefore the critical exponents independent of the density fermions at $n > 2/3$. For $J > J_0$ K_ρ decreases with n and reaches a minimal value $4/9$ at half-filling, the value of K_ρ decreases with J also. The value of Θ increases and reaches a maximum value 0.37 at half-filling, both phases are dielectric for $J > 2$ at $n \geq 2/3$. At half-filling the value $J = 2$ separates the phase of itinerant fermions on gapless at $J \leq 2$ and gaped at $J > 2$. The behavior of the density of the magnetization as a function of the magnetic field, calculated for different values of the interaction J , is shown in Fig. 5. The magnetization of the system has a jump at $H=0$ equal to $1/3$. This jump corresponds to the phase of frozen fermions with the chemical potential equal to zero.

In summary, we presented the exact phase diagram of the zig-zag ladder model for arbitrary Coulomb repulsion interaction and density of fermions obtained on the basis of the exact solution of the model. It is shown that intrinsic effective attractive hard-core interaction and Coulomb repulsion form the Luttinger liquid state in the ladder. Due to special role of the effective attractive hard-core interaction, two phases of the itinerant and frozen fermions are separated at the high density, when filling exceeds $2/3$. As a result, the system exhibits two types of behavior in high density region: either band insulator in the case of the strong interaction at $J > 2$ or the Luttinger liquid state for one phase and band insulator for another at $J \leq 2$. The values of bulk exponents calculated in the framework of the model adopted are in a reasonable agreement with the measurements in SWNT's.

The author wishes to thank the support of the Visitor Program of the Max-Planck-Institut für Physik Komplexer Systeme, Dresden, Germany. Part of this work was performed at the International Centre for Theoretical Physics, Trieste, Italy. Research supported by the Nano Structure Systems, Nano materials and Nano Technology Program, project STSU-3520.

¹ H. Ishii *et al.*, Nature (London) **426**, 540 (2003).

² A. Bachtold, M. de Jonge, K. Grove-Rasmussen, P. L. McEuen, M. Buitelaar and C. Schenberger, Phys. Rev. Lett. **87**, 166801 (2001).

³ M. Bockrath *et al.*, Nature (London) **397**, 598 (1999).

⁴ R. Egger and A.O. Gogolin, Eur. Phys. J. B **3**, 281 (1997); R. Egger, Phys. Rev. Lett. **83**, 5547 (1999); C. Kane, L. Balents, and M.P.A. Fisher, Phys. Rev. Lett. **79**, 5086 (1997).

⁵ I.N. Karnaukhov, V.I. Kolomytsev, and C.G.H. Diks, Phys. Rev. B **75**, 125407 (2007); I.N. Karnaukhov and A.A. Ovchinnikov, Europhys. Lett. **57**, 540 (2002).

⁶ R. Saito, G. Dresselhaus, and M.S. Dresselhaus, *Physical Properties of Carbon Nanotubes* (Imperial College Press, London, 1998).

⁷ Z. Wihong, V. Kotov, and J. Oitmaa, Phys.Rev. B **57**,

11439 (1998); X. Wang, Mod. Phys. Lett. B **14**, 327 (2000);

T. Hakobyan, Phys.Rev. B. **75**, 214421 (2007).

⁸ H. Frahm, M. Pfannmüller, and T.M. Tsvelik, Phys. Rev. Lett. **81**, 2116 (1998).

⁹ A.A. Nersesyan and A.M. Tsvelik, Phys. Rev. B **68**, 235419 (2003).

¹⁰ D.N. Aristov, M.N. Kiselev, and K. Kikoin, Phys. Rev. B **75**, 224405 (2007).

¹¹ Y. Wang, Phys. Rev. **60**, 9236 (1999); M.T. Batchelor and M. Maslen, J.Phys. A **32**, L377 (1999); H. Frahm and C. Rödenbeck, J. Phys. A., **30**, 4467 (1999); H. Frahm and A. Kundu, J.Phys. Condens. Matter **11**, L557 (1999); P. Corboz, A.M. Läuchli, K. Totsuka, and H. Tsunetsugu / cond-mat.0707.1195 (9 July 2007).